

Ventricular stroke work and efficiency both remain nearly optimal despite altered vascular loading

PIETER P. DE TOMBE, STEVEN JONES, DANIEL BURKHOFF,
WILLIAM C. HUNTER, AND DAVID A. KASS

*Division of Cardiology, Departments of Internal Medicine and Biomedical Engineering,
The Johns Hopkins Medical Institutions, Baltimore, Maryland 21205*

De Tombe, Pieter P., Steven Jones, Daniel Burkhoff, William C. Hunter, and David A. Kass. Ventricular stroke work and efficiency both remain nearly optimal despite altered vascular loading. *Am. J. Physiol.* 264 (*Heart Circ. Physiol.* 33): H1817-H1824, 1993.—Recent clinical and animal studies have suggested that ventricular-vascular coupling normally operates at either optimal ventricular efficiency (EFF = stroke work/myocardial oxygen consumption) or stroke work (SW) and that efficiency in particular is compromised by cardiac dysfunction. These distinctions between coupling states at maximal work vs. efficiency are largely based on theoretical models. To date, there are few direct experimental data defining optimal conditions for each parameter, respectively, in the same heart or tests of whether changes from these conditions must produce significant declines in both parameters. Therefore, 10 isolated blood-perfused canine hearts were studied at varying contractilities, with the heart ejecting into a simulated three-element Windkessel model of arterial impedance. For a given inotropic state [indexed by the slope of the end-systolic pressure-volume relationship (E_{es})], myocardial oxygen consumption and SW were measured over a broad range of afterload resistances. The latter was indexed by the effective arterial elastance (E_a) and ventricular-vascular interaction expressed by the ratio of E_a to E_{es} (E_a/E_{es}). On average, maximal SW occurred at $E_a/E_{es} = 0.80 \pm 0.16$, whereas EFF was maximal at $E_a/E_{es} = 0.70 \pm 0.15$ ($P < 0.01$). However, these differences were small, and both SW and EFF were $\geq 90\%$ of their respective optima over a broad overlapping range of E_a -to- E_{es} ratios (0.3–1.3, corresponds with ejection fractions ranging from ~ 40 to 80%). These data show that both SW and efficiency are nearly maximal under many conditions of ventricular-vascular interaction. This suggests that precise optimization of either parameter is unlikely to be a major target of cardiovascular homeostasis under many circumstances.

pressure-volume relations; energetics; ventriculo-arterial matching; contractility; heart function; left ventricle

EXPERIMENTAL AND THEORETICAL analyses of left ventricular coupling with the arterial vascular system have yielded several hypotheses regarding the primary factors that control this interaction (3, 6). It is generally accepted that vascular properties and hemodynamic requirements are dictated by organism size and that ventricular size and strength adjust to provide the required systemic blood flow and pressure in an optimal manner (6). Theories differ with regard to what is believed to be optimized. Studies in isolated and intact animal hearts suggest that vascular and ventricular properties are matched to achieve maximal transfer of mechanical energy (6, 12, 25–27) (i.e., power or stroke work). Alternatively, theoretical analysis as well as data from conscious animals and humans suggest that ventricular metabolic efficiency, defined as the ratio of stroke work to myocardial oxygen consumption per beat, may be optimized under normal conditions (1, 3, 9, 14, 18).

These distinctions may have clinical relevance (1, 9, 19). Studies have suggested that cardiac efficiency is compromised in human congestive heart failure in favor of maximal external work, whereas the opposite appears the case in normal hearts (1, 19). Therapeutic interventions such as vasodilator therapy can thus be viewed with respect to their capacity to improve efficiency (9, 14, 15). This notion is appealing, particularly if energy delivery to the heart is compromised. Unfortunately, although conditions for maximal stroke work or power have been extensively studied (6, 12, 14, 25–28), simultaneous metabolic data are scant (5, 20, 26). The data that exist do not clearly define conditions for which efficiency is maximal, or even whether there is an optimum (20). Thus prior interpretations of clinical ventricular-vascular data have primarily been based on model predictions rather than measured data.

For the distinction between coupling states at maximal work vs. efficiency to be meaningful, optimal conditions must be reasonably different, and any change from these conditions should produce a significant decline in one or the other parameter. The present study directly tested these features by simultaneously measuring mechanical and energetic data in isolated blood-perfused canine left ventricles contracting against a computer-simulated vascular load. Although the results confirm that each parameter is optimal at different conditions of ventricular-vascular interaction, this difference is found to be quite small. Furthermore, both parameters remain near maximal over a broad overlapping range of interaction.

METHODS

Surgical preparation. Ten isolated canine ventricles were studied. The procedures used to isolate and support the canine heart have been previously described in detail (17, 22). Briefly, two mongrel dogs (25–35 kg) anesthetized with pentobarbital sodium (30 mg/kg) were used for each experiment. The support dog was premedicated with hydrocortisone (500 mg im), diphenhydramine (50 mg), indomethacin (25 mg pr), and heparin (5,000 IU). The femoral arteries and veins of the support dog were cannulated to provide perfusion of oxygenated blood to a heart isolated from a second (donor) dog. The chest of the donor dog was opened under artificial ventilation. The subclavian artery and right atrium were cannulated and connected to the perfusion system. The heart was then isolated under continuous blood perfusion, with temperature controlled at 37°C. The left ventricle (LV) was vented, the left atrium opened, and all chordae tendineae were cut. A ring adapter was sewn into the mitral annulus, and a thin latex balloon connected to a volume control system was placed within the LV chamber. Left ventricular pressure was measured inside the balloon by a micro-manometer (PC-380, Millar, Houston, TX). A bipolar surface

electrocardiogram was obtained from two surface electrodes sutured to the LV.

Coronary perfusion pressure was measured via a catheter placed through the brachiocephalic trunk into the aortic root. Two perfusion pumps (model 1215, Harvard Apparatus, South Natick, MA) maintained mean coronary perfusion pressure at 80 mmHg (2). The first pump withdrew arterial blood from the support dog at a constant rate while the second pump diverted blood flow so as to bypass the isolated heart. This arrangement maintained a fixed hemodynamic demand on the support dog, independent of coronary flow to the isolated heart, which helped stabilize the preparation. The support dog was also mechanically ventilated, and blood pH, PO_2 , and PCO_2 were maintained in the normal range by adjustment of ventilation rate. The support dog was administered sodium bicarbonate and O_2 as required.

The right ventricle and atrium of the isolated heart were drained via a wide-bore cannula with side holes. The right heart was made airtight by purse string suture around the cannula at the right ventricle apex and ligation of superior and inferior venae cavae. Total coronary blood flow (excluding a small amount of LV thebesian flow) was measured by draining all blood from the right heart via an in-line ultrasonic flow probe (Transonics, Ithaca, NY). The difference in oxygen content between arterial and coronary venous blood (AVO_2) was continuously measured by absorption spectrophotometry (AVOX-Systems), which was calibrated to an oxygen analyzer (I.F.X.- O_2 -Con). Total heart oxygen consumption (MVO_2) was calculated as the product of coronary blood flow and AVO_2 .

In seven hearts, heart rate was fixed by atrial pacing at 10–15 beats/min above the spontaneous atrial rate. In three studies, atrioventricular conduction block was induced by injecting 10% Formalin solution (0.1–0.3 ml) into the atrioventricular node; hearts were then paced at the LV apex at 90 (2 dogs) and 100 min^{-1} (1 dog).

Hearts contracted against a computer-simulated vascular loading system (three-element windkessel) consisting of a characteristic impedance (R_c), peripheral arterial resistance (R_a), and arterial compliance (C_a). Ventricular filling during diastole was accomplished by a simple computer-simulated circuit, consisting of a pressure source and resistance. The design and implementation details of this servo system have been previously reported, and the reader is directed to these studies for a full description (17, 23, 24).

Experimental protocol. After the preparation was completed, each heart was provided 20 min for stabilization. The primary aim was to assess sensitivities of ventricular efficiency and stroke work (SW) to changes in ventricular and arterial properties. This was achieved by varying the simulated arterial resistance over a broad range at constant left ventricular "contractility," heart rate, and end-diastolic volume (EDV). Ventricular systolic properties were indexed by the slope of the end-systolic pressure-volume relationship (17, 22) (E_{es}). Vascular loading was indexed by the effective arterial elastance (E_a) (24, 25). E_a is approximately equal to the total mean arterial resistance divided by cardiac cycle length (24, 25). These two parameters were used to determine a ventricular-to-vascular coupling ratio (E_a/E_{es}), as previously described by Sunagawa and colleagues (25). To guarantee that a sufficient range of coupling ratios was assessed in each heart, E_{es} was first estimated (from isovolumic beats at varying volumes), and using known cycle length, eight or more R_a values were predetermined that would yield E_a -to- E_{es} ratios approximately between 0.3 and 8.0. These R_a values were then randomly selected and entered into the computer vascular loading model. R_c was held constant (0.2 $mmHg \cdot ml^{-1} \cdot s$), and C_a was adjusted so that the diastolic decay time constant ($R_a \cdot C_a$) was fixed at 1.3 s. This latter step ensured that the pressure-volume loops had fairly well-defined

diastolic and systolic corners at each of the selected afterloads. Two to three minutes of equilibration were provided between each randomly selected E_a value. In summary, for each experimental run, data were measured at the preselected afterload conditions with constant heart rate and EDV (Fig. 1). At each load, left ventricular pressure and volume, coronary perfusion pressure and flow, myocardial arteriovenous oxygen difference (AVO_2), and surface electrocardiogram were recorded. After a complete loading sequence was obtained, cardiac conditions were changed either by switching to a smaller or larger EDV (~50% change) or inotropic state (intracoronary infusion of dobutamine at 1–5 $\mu g/min$ or $CaCl_2$ at 1–5 $mmol/min$). After a new steady-state condition was achieved, the protocol was repeated. In this manner, a total of 31 separate variable afterload runs were obtained from the 10 hearts. Data sufficient to define optimal coupling for both SW and efficiency were obtained in 26 (80%) of the afterload runs. Failure in the remaining five was due to inadequate data collection at low coupling ranges (≤ 0.5) stemming from limitations in volume servo system at low afterload resistances (requiring large volume displacements), particularly in hearts with rapid heart rates and low E_{es} . These data could not be used to analyze for differences in the coupling ratio at optimal work vs. efficiency but were examined.

Data signals were digitized at 200 Hz and stored on diskettes for off-line analysis. At the end of the experiment the weights of the right ventricular free wall and the LV (including the septum) were measured.

Data analysis. The principal relations were those between SW or efficiency and the coupling ratio E_a to E_{es} . The E_{es} values used to determine this ratio for each loading condition were derived from each respective set of ejecting beats at varying afterload (i.e., Fig. 1). The end-systolic pressure-volume relationship was defined by the locus of points of the ratio maximal pressure to volume – V_o , with volume axis intercept (V_o) determined with use of an iterative technique (17). Data were fit by linear regression with slope E_{es} . This approach assumes that afterload change in and of itself does not alter E_{es} . This is a simplification, since we recently demonstrated that afterload can modestly alter E_{es} (2). The potential impact of this simplification on the data is discussed later.

E_a was calculated for each pressure-volume loop as the ratio of end-systolic pressure (P_{es}) to stroke volume ($SV = V_{max} - V_{min}$, where V_{max} and V_{min} are maximum and minimum volume, respectively). SW was the numerically integrated area within each loop. Total mechanical work was measured by the pressure-volume area (PVA) as described by Suga et al. (11, 21). PVA was calculated by determining the area bounded by the

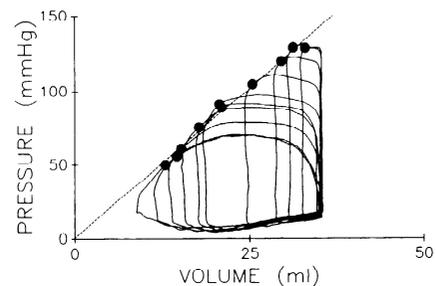


Fig. 1. Example of experimental protocol. Left ventricular pressure is plotted as function of instantaneous left ventricle volume. Ventricles were made to "eject" against different levels of computer-simulated arterial afterload resistance (10 levels in this example). End-systolic pressure-volume coordinates are indicated by solid circles and fit to equation: $P_{es} = E_{es}(V_{es} - V_o)$ (dashed line), where P_{es} is end-systolic pressure, E_{es} is end-systolic elastance and equals 4.05 $mmHg/ml$, and V_o is volume axis intercept and equals -0.2 ml; $r = 0.991$. For each beat, area within pressure-volume loop [stroke work (SW)], myocardial oxygen consumption (MVO_2), and arterial load were determined.

end-systolic pressure-volume relationship and diastolic pressure-volume relationship and the systolic trajectory of the pressure-volume loop. All steady-state mechanical and energetic parameters were derived from an average of 4-6 sequential cardiac cycles.

Per beat total $\dot{M}\dot{V}O_2$ was obtained by dividing $\dot{M}\dot{V}O_2$ measured at each afterload by heart rate. LV $\dot{M}\dot{V}O_2$ was equal to total heart $\dot{M}\dot{V}O_2$ minus the O_2 consumption of the unloaded right ventricle. The latter was estimated by multiplying the unloaded $\dot{M}\dot{V}O_2$ of the whole heart by the ratio of right ventricle to total heart mass. Myocardial efficiency was defined as the ratio of SW to $\dot{M}\dot{V}O_2$ ($SW/\dot{M}\dot{V}O_2$), with both measures first converted into joules per beat ($1 \text{ ml } O_2 = 20 \text{ J}$; $1 \text{ mmHg/ml} = 1.334 \cdot 10^{-4} \text{ J}$). The result was expressed as a percent.

Statistical analysis. To determine the E_a -to- E_{es} ratio at maximal SW and efficiency ($SW/\dot{M}\dot{V}O_2$), data from each experimental run were fit by nonlinear regression to a Gaussian function of the form: SW (or $SW/\dot{M}\dot{V}O_2$) = $k \cdot e^{-((\ln[E_a/E_{es}] - \mu)/\sigma)^2}$, where $\mu = \ln(E_a/E_{es})$ at the point of maximal SW or efficiency (μ and σ are constants). Although this choice of fit was somewhat arbitrary, it both characterized the data well and provided a simple and direct method to estimate the optimal point. The adequacy of the nonlinear fit was indicated by the $1 - \text{RSS-to-CSS}$ ratio, where RSS and CSS are the residual and corrected total sum of squares, respectively. The mean value of this ratio was 0.91 ± 0.096 . Comparisons of μ values derived from the Gaussian fits were made by paired t testing (13). The pooled data were also fit to a Gaussian function. Statistical analyses, including linear and nonlinear regressions, were performed using commercial software (SYSTAT, Evanston, IL). Data are presented as means \pm SD. Where appropriate, paired or unpaired Student's t test was used for comparisons, with significance accepted at the $P < 0.05$ level.

RESULTS

Figure 2 displays an example of SW and metabolic efficiency ($SW/\dot{M}\dot{V}O_2$) vs. R_a (Fig. 2, left) and the same variables vs. coupling ratio (E_a/E_{es} ; Fig. 2, right) for a typical heart. The corresponding bottom panels display the same data on a semilogarithmic scale, with each variable normalized to its optimal value. Plots as functions of R_a are shown, since this was the principal independent variable. Characterization of this change by the E_a -to- E_{es} ratio enabled adjustment for between run and interheart variations in contractile state, thus facilitating group data analysis. As shown in Fig. 2, the two representations yielded virtually identical qualitative results. Both SW and efficiency demonstrated clear optima at coupling ratios slightly below 1.0 (resistance of 1.2 mmHg/ml or 1,600 dyn \cdot s \cdot cm $^{-5}$). Maximal metabolic efficiency was 8.5% in this example, typical of the data overall ($9.4 \pm 5.6\%$). The semilogarithmic plots more clearly demonstrate the broad range of coupling ratios (and resistances) over which both variables are optimal. The curves in these lower plots are the Gaussian fits to the data.

Table 1 provides data for a typical data run for each heart. Absolute values for SW, efficiency, calculated mean arterial pressure, and $\dot{M}\dot{V}O_2$ at optimal work are given, along with ranges for these and other parameters obtained by varying resistance. E_{es} values span a somewhat broader and higher range than typical of isolated hearts, reflecting inotropic support provided by intracoronary infusion of $CaCl_2$ or dobutamine (see METHODS).

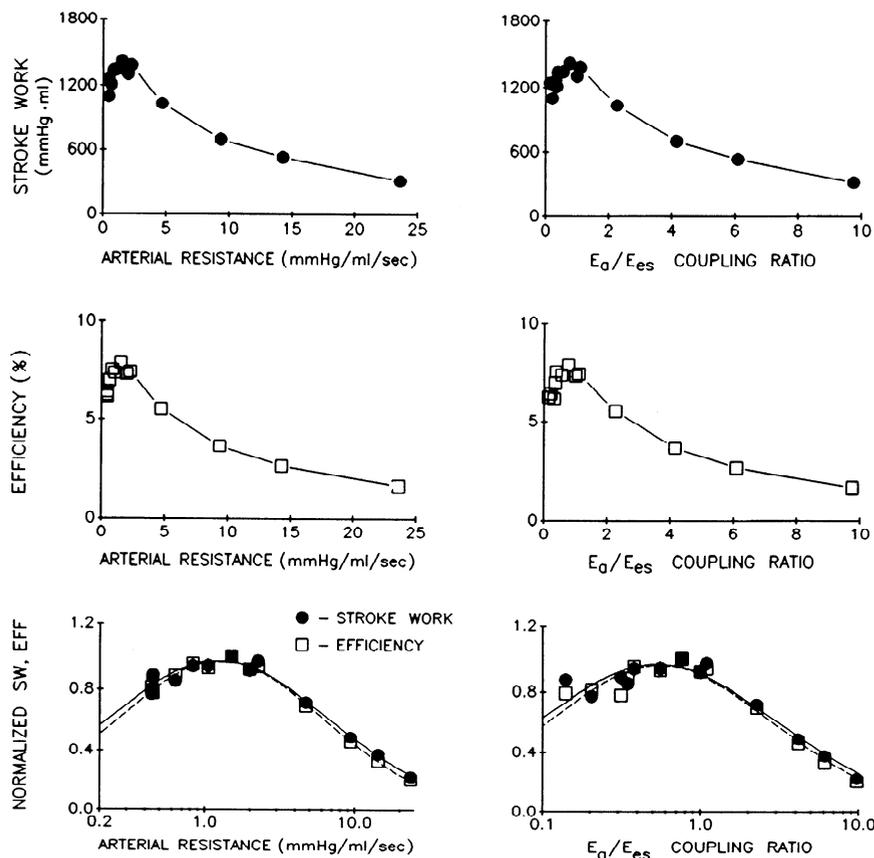


Fig. 2. SW and efficiency as function of resistance or arterial elastance (E_a)-to- E_{es} ratio (E_a/E_{es}). Left: SW and metabolic efficiency [ratio of SW to $\dot{M}\dot{V}O_2$ ($SW/\dot{M}\dot{V}O_2$)] as functions of arterial resistance. Right: same 2 variables as functions of effective E_a normalized to ventricular E_{es} (E_a/E_{es}). Bottom panels: replot of respective left and right column data on a semilogarithmic scale with data normalized to their respective maximum. Plots of each variable vs. resistance or E_a -to- E_{es} coupling ratio were qualitatively virtually identical. Both variables demonstrate clear optima, and there is considerable overlap (most easily discerned in semilog plots) and a broad peak to both relations. SW, EFF, stroke work and efficiency.

Table 1. Values for hemodynamic parameters measured at low and high resistances and at maximal stroke work, and peak efficiency obtained in a representative data run for each heart

Dog	HR, min ⁻¹	$E_{es}/100$ g, mmHg·ml ⁻¹ ·100 g ⁻¹	Range of Resistance and Hemodynamic Parameters*					Measured at Maximal Stroke Work		Peak efficiency, %
			Resistance, mmHg·ml ⁻¹ ·s	SV, ml	SW, mmHg/ml	mABP, mmHg	$M\dot{V}O_2$, ml O ₂ ·min ⁻¹ ·100 g ⁻¹	mABP, mmHg	$M\dot{V}O_2$, ml O ₂ ·min ⁻¹ ·100 g ⁻¹	
1	150	5.3	0.67-14.5	20.4-3.7	1,860-519	34-134	0.0988-0.1137	79	0.1129	11.8
2	167	9.4	0.41-5.4	25.5-9.2	2,207-1,350	29-138	0.1170-0.1550	75	0.1370	10.7
3	128	5.0	0.34-11.7	32.6-5.1	2,217-569	24-127	0.1594-0.1975	58	0.1818	8.3
4	133	6.1	0.33-11.2	27.4-4.7	1,534-471	20-117	0.0415-0.0515	68	0.0506	22.9
5	90	7.0	0.77-11.9	28.7-8.2	2,336-1,232	33-146	0.1527-0.1809	58	0.1668	9.3
6	136	14.7	0.18-16.5	12.4-3.0	899-337	21-112	0.1892-0.2000	72	0.1967	2.6
7	150	11.0	0.44-5.6	20.4-8.5	1,592-584	21-119	0.1594-0.2897	64	0.2897	3.7
8	90	3.9	0.53-19.0	26.0-2.7	1,264-195	21-77	0.1270-0.1536	31	0.1336	6.3
9	100	6.9	0.44-23.6	26.8-3.1	1,421-321	20-122	0.1137-0.1369	50	0.1195	7.9
10	150	14.8	0.26-3.7	29.1-4.7	2,163-1,729	19-136	0.1237-0.1718	76	0.1378	10.8
Mean	129.4	8.4	0.437† 12.3‡	24.9† 5.3‡	1,749† 730.7‡	24.2† 122.8‡	0.1282† 0.1520‡	63.1	0.1526	9.4
±SD	±27.3	±3.9	±0.18 ±6.3	±5.8 ±2.5	±482 ±516	±5.6 ±19.3	±0.041 ±0.044	±14.6	±0.629	±5.6

HR, heart rate; E_{es} , end-systolic elastance; SV, stroke volume; SW, stroke work; mABP, mean arterial blood pressure; $M\dot{V}O_2$, myocardial oxygen consumption. The broad range of E_{es} reflects the use of intracoronary inotropic support. * Minimum and maximum resistances are provided along with corresponding SV, SW, mABP, and $M\dot{V}O_2$ values measured at these resistances. † Mean ± SD of low parameters; ‡ mean ± SD of high parameters.

In most cases, these values were not that dissimilar from what is observed in more intact preparations.

Gaussian relations were fit to the data obtained from each afterload run ($n = 26$) to determine coupling ratios at optimal SW vs. efficiency. There was a small but significant difference between the loading conditions (coupling ratio) at each optimum, with maximal SW/ $M\dot{V}O_2$ occurring at a lower afterload resistance relative to E_{es} (E_a -to- E_{es} ratio = 0.696 ± 0.15) than SW (0.80 ± 0.16 , $P < 0.0001$). Figure 3 displays the E_a -to- E_{es} ratio at peak SW vs. peak efficiency for each data run. Whereas most data points fell above the identity line (greater coupling ratio at maximal SW), this difference was frequently very small.

Pooled data with mean Gaussian fits are displayed in Fig. 4. Each run was normalized to its optimal value (defined by nonlinear fit). As was true for individual runs, pooled data also yielded a significantly larger coupling ratio of 0.77 (95% confidence interval: 0.73-0.81) for

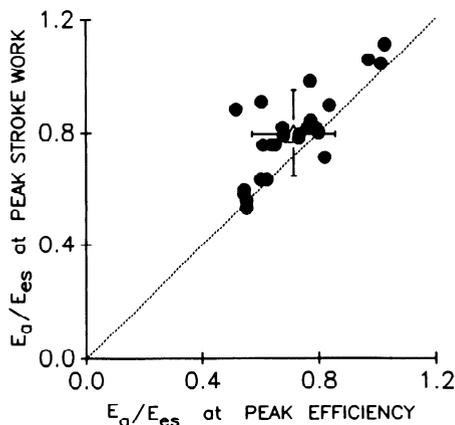


Fig. 3. Optimum E_a -to- E_{es} ratio for SW vs. efficiency. Comparison of E_a/E_{es} at maximal SW vs. metabolic efficiency. Optimal ratios were determined from Gaussian fits to each experimental run (see METHODS). Dashed line, line of identity; open triangle, mean ± SD for all experiment runs. Majority of data fell above line of identity ($P < 0.001$), indicating a greater E_a -to- E_{es} ratio at maximal SW vs. efficiency.

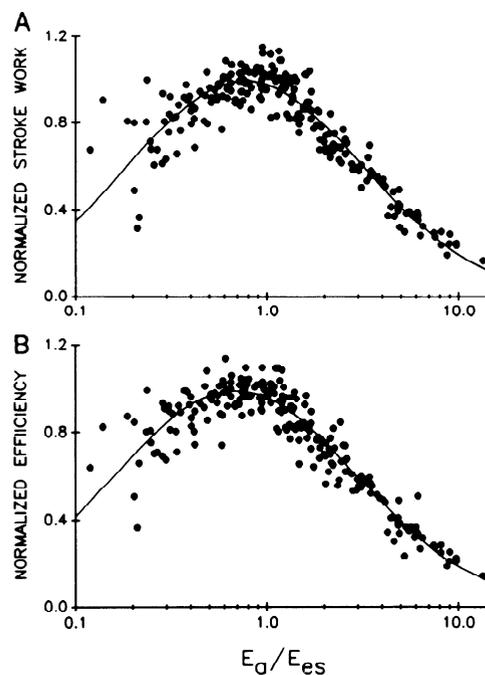


Fig. 4. SW and efficiency as function of E_a/E_{es} (group data). Data were normalized in each experimental run to maximum SW (A) or maximum efficiency (B). Pooled data from 26 experimental runs obtained in 8 hearts are shown ($n = 220$). Pooled data were again fit to a Gaussian function (solid line) to determine E_a -to- E_{es} ratio at maximum SW or SW/ $M\dot{V}O_2$. Maximal SW was observed at E_a -to- E_{es} ratio = 0.75 (95% confidence interval: 0.71-0.80) for maximal SW vs. 0.638 (0.60-0.68) for maximal SW/ $M\dot{V}O_2$ ($P < 0.05$).

maximal SW vs. 0.685 (0.65-0.72) for maximal SW/ $M\dot{V}O_2$ ($P < 0.05$). Although maximal SW and efficiency occurred at slightly different afterloads, there was considerable overlap. This is more directly depicted by averaged relations determined from the group data (Fig. 5). Portions of each relation that fall at or above the dotted line in Fig. 5 delineate the range of coupling ratios at which both work and efficiency were $\geq 90\%$ of optimal. This range was broad, spanning an E_a -to- E_{es} ratio of

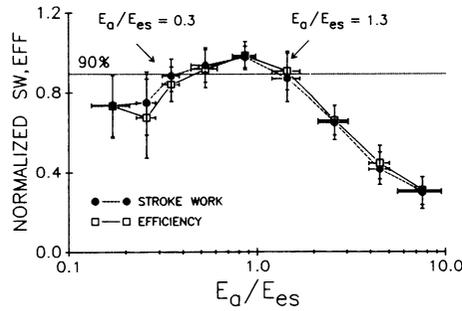


Fig. 5. Average normalized SW and SW/M $\dot{V}O_2$ as a function of E_a/E_{es} . Data from Fig. 4 were averaged over equipaced bins of E_a -to- E_{es} ratios and are displayed on a semilogarithmic plot. Dotted line, range of coupling ratios above which SW and SW/M $\dot{V}O_2$ are $\geq 90\%$ of optimal. Note that this range was broad, spanning an E_a -to- E_{es} ratio of 0.3–1.3 and that optimum for both SW and efficiency were close. Mean \pm SD bars are shown and were smaller than symbol size at higher coupling ratios.

0.3–1.3 and includes values that have been reported both for normal human hearts (near 0.6) (1, 9, 19) and conscious dogs (near 1.0) (12), as well as in acute cardiac depression and human cardiomyopathy (near 1.3) (1, 9). This coupling range translates into an ejection fraction range from ~ 40 to 80%.

Impact of E_{es} and EDV. The 26 individual relations relating SW or SW/M $\dot{V}O_2$ to E_a -to- E_{es} ratio were obtained in hearts at varying preload volumes, heart rates, and contractilities, as summarized in Table 2. Prior theory and experimental data from the isolated heart has shown that neither EDV, E_{es} , nor heart rate alters the coupling ratio at maximal SW (3, 25). However, analogous data for efficiency do not exist, although theory predicts an influence (3, 10). Therefore, we assessed these dependencies in the present data using the following multiple linear regression model: E_a -to- E_{es} ratio at maximal SW (or SW/M $\dot{V}O_2$) $_{max} = b_0 + b_1 \times EDV + b_2 \times E_{es} + b_3 \times HR$, where HR is heart rate. Results are provided in Table 3. This analysis confirmed the lack of sensitivity of coupling ratio at maximal SW to EDV, HR, or E_{es} . However, for efficiency, there was a significant negative dependence on E_{es} . Thus the E_a -to- E_{es} ratio at maximal efficiency was lowest at high contractilities and increased (getting closer to that for optimal SW) at reduced contractility.

DISCUSSION

The interaction between the heart and the vascular loading system determines the external work and metabolic efficiency with which the heart performs that work. Prior theoretical and some experimental data suggested that work and efficiency could not both be maximized under a given set of conditions. Extension of these con-

Table 3. Multiple regression analysis of effect of EDV, E_{es} , and HR on the E_a -to- E_{es} ratio at maximal SW and efficiency

Parameter	Coefficient	P
SW		
Constant	0.802 \pm 0.208	0.001*
EDV	-0.002 \pm 0.004	0.657
E_{es}	-0.009 \pm 0.008	0.260
HR	0.001 \pm 0.001	0.436
Efficiency (SW/M $\dot{V}O_2$)		
Constant	0.985 \pm 0.180	0.001*
EDV	-0.003 \pm 0.004	0.380
E_{es}	-0.018 \pm 0.007	0.012*
HR	0.000 \pm 0.001	0.802

SW/M $\dot{V}O_2$, ratio of SW to M $\dot{V}O_2$, E_a , arterial elastance. Data were fit by multiple linear regression to E_a -to- E_{es} ratio at maximal SW (or SW/M $\dot{V}O_2$) = $b_0 + b_1 \cdot EDV + b_2 \cdot E_{es} + b_3 \cdot HR$ to test for the influence of EDV (b_1), E_{es} (b_2), and HR (b_3) on the E_a -to- E_{es} coupling ratio at optimal SW or SW/M $\dot{V}O_2$ (b_0 is a constant). * $P < 0.05$ by multiple linear regression.

cepts to intact human subjects has led to the notion that precisely which parameter is maximal may have both clinical and therapeutic significance (1, 9, 15, 19). The present data appear to weaken this notion. Although work and efficiency are indeed optimized at slightly different afterload resistances (work peaking at a slightly higher resistance than SW/M $\dot{V}O_2$), this difference is generally small. Furthermore, the sensitivity of both parameters to changes in resistance is sufficiently low that both parameters can exceed 90% of their respective maximal values over a broad loading range. Thus, under physiological and even some pathophysiological states, both parameters remain near optimal.

Ventricular efficiency optimization. To our knowledge this is the first study in which an optimum for metabolic efficiency (SW/M $\dot{V}O_2$), as function of R_a , has been measured. Early studies of loading effects on cardiac efficiency were performed by Sarnoff and co-workers (18), although the artificial loading methods used made this data difficult to interpret. A more recent study was reported by Elzinga and Westerhof (5) in isolated cat hearts, in which ventricular and arterial properties were defined by mean pressure-flow relations. Elzinga and Westerhof (5) found that work and efficiency were optimized at different mean flows. However, the lower R_a range was limited in this study, since arterial and coronary perfusion pressure were dependent on the pumping action of the left heart. Consequently, M $\dot{V}O_2$ data were not obtained at sufficiently high flows to define the optimal point of metabolic efficiency in most of the hearts. This was not a problem in the present study, since coronary perfusion was independently controlled. Furthermore, by maintaining heart rate in a more physiological range in many hearts, we were able to reduce arterial impedance sufficiently for more direct determination of conditions at optimal efficiency in nearly 80% of the experiments.

Prior experiments have shown (26), and theory predicts (3), that the ventricular-arterial coupling conditions (E_a/E_{es} rates) at maximal SW are independent of EDV or contractile state (E_{es}). This was found in the present

Table 2. Range of cardiac size and systolic function

	Mean \pm SD	Range
E_{es} , mmHg \cdot ml \cdot 100 g^{-1}	8.89 \pm 4.68	3.46–24.9
EDV, ml	25.7 \pm 9.5	7.9–41.1
HR, min^{-1}	126.3 \pm 27.3	85–167
Mass $_{LV}$, g	143.8 \pm 20.4	112–172
Mass $_{RV}$, g	54.5 \pm 3.0	42–72.3

EDV, end-diastolic volume; Mass $_{LV}$, Mass $_{RV}$, mass of left ventricle and right ventricle, respectively.

study as well. Similar analysis also predicts the opposite to be the case for coupling at peak ventricular efficiency (3, 10). The present data are the first to confirm this experimentally, showing a significant negative correlation between the E_a -to- E_{es} ratio at peak efficiency and contractile state (E_{es}). This indicates that as the contractile state of the heart is decreased, the coupling ratio at optimal SW and efficiency converge, consistent with the model prediction (10). This runs counter to the notion that an increase in E_a -to- E_{es} ratio with heart failure necessarily indicates that the heart is working further away from optimal efficiency in favor of external work, as suggested by recent studies (1, 9, 19). Rather, this observation raises the possibility that both normal and moderately diseased ventricular-arterial coupling may occur without critically compromising either cardiac work or efficiency.

Myocardial efficiency is often defined in several ways (11, 15, 21). This study focused on a common definition that varies with afterload resistance, namely the $\dot{M}\dot{V}O_2$ cost of delivering SW. This is not to imply that metabolic efficiency of cardiac chemomechanical energy conversion is similarly variable. Rather a variable amount of the mechanical energy generated by the ventricle is liberated to perform external work, whereas the remaining mechanical "potential" energy is presumably dissipated as heat (11, 21). This explains the relatively low efficiencies as given in Table 1. The sum of both internal potential energy and SW work yields PVA, which is linearly related to $\dot{M}\dot{V}O_2$ (11, 17, 21). The inverse slope of this relation is cardiac chemomechanical conversion efficiency and is relatively insensitive to arterial load. In the present study, this efficiency averaged $27.1 \pm 12.4\%$, similar to prior data from our laboratory (2).

Yet another form of efficiency, called work efficiency, relates external work to total potential external work (i.e., PVA) (7, 12, 15, 19). This has become popular, particularly in clinical studies, due to the relative ease of measuring PVA as opposed to $\dot{M}\dot{V}O_2$ in vivo. Unlike $SW/\dot{M}\dot{V}O_2$, which is optimized at a physiological resistance, the SW-to-PVA ratio increases monotonically with declining afterload and is maximal at zero load. Thus this ratio is never "optimized" except at a non-physiological load. This is demonstrated in Fig. 6, which compares the two efficiency ratios as functions of the E_a -to- E_{es} ratio, both derived from the present data. The SW-to-PVA ratio yields a lower coupling ratio for "maximal" efficiency than that obtained from $SW/\dot{M}\dot{V}O_2$. This likely contributed to greater apparent disparities in loading conditions for maximal SW vs. SW/PVA (9, 12, 19) compared with what we report for SW vs. $SW/\dot{M}\dot{V}O_2$. In absolute terms, the SW/PVA is also much greater than $SW/\dot{M}\dot{V}O_2$ (averaging $76.0 \pm 6.7\%$ in the present study) because it ignores the $\dot{M}\dot{V}O_2$ costs of excitation-contraction coupling and basal metabolism. For all these reasons, we do not believe it is a particularly useful efficiency expression.

Comparison with prior data. The coupling ratio at optimal SW reported in the present study is somewhat lower than previously reported by Sunagawa et al. (25), although similar to that observed in conscious animals

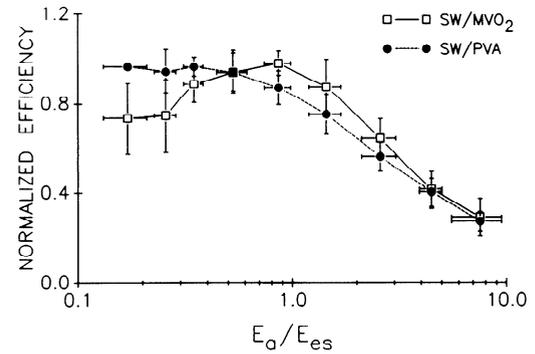


Fig. 6. Average normalized $SW/\dot{M}\dot{V}O_2$ vs. SW-to-pressure-volume area (PVA) ratio as function of E_a/E_{es} . Comparisons are made between 2 definitions of ventricular efficiency. One is ratio of SW to $\dot{M}\dot{V}O_2$ used in present study. Another, termed work efficiency, is given by ratio of SW to total PVA (SW/PVA). This latter efficiency, unlike $SW/\dot{M}\dot{V}O_2$, has no optimum as a function of ventricular-vascular coupling ratio (E_a/E_{es}), but rather, continues to rise with reduced arterial loading. As in Fig. 5, means \pm SD are shown.

(13). Theoretical analysis predicts that maximal work occurs when ventricular and effective E_a s are matched, i.e., $E_a/E_{es} = 1.0$. This analysis depends on there being little deviation of ejection pressure from the mean (i.e., pressure-volume loop looks like a box) and that diastolic pressure can be ignored. Although the pressure-volume loops in the present study were generally close to a "box" appearance, this was less so at very low and high resistances (see Fig. 1). Specifically, at low loads, SW tended to be greater than theoretically predicted, likely explaining the finding that the E_a -to- E_{es} ratio at optimal SW was slightly less than unity. This disparity can be quantified by comparing an estimated P_{es} (SW-to-SV ratio), which gives the average height of the pressure-volume loop, assuming a boxlike shape, to measured P_{es} . This is shown in Fig. 7. In the upper loading range (high

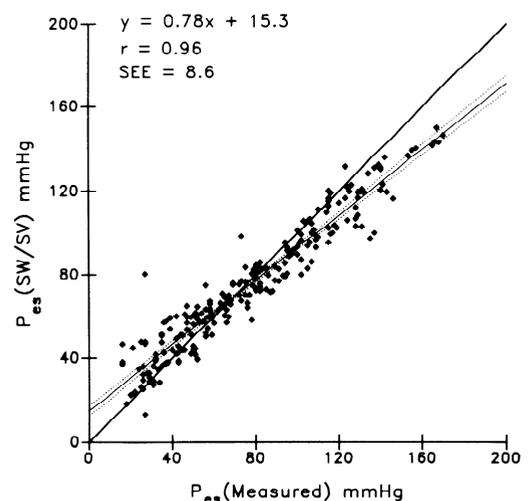


Fig. 7. Measured P_{es} vs. P_{es} estimated if pressure-volume loop is box shaped. Actual P_{es} compared with value that is assumed by E_a -to- E_{es} coupling model, based on a simplified boxlike shape of pressure-volume loop. Latter is estimated by dividing measured SW by stroke volume. In upper pressure range, measured P_{es} exceeded P_{es} assumed by coupling model, whereas opposite was true in lower range. Crossover occurred near 80 mmHg. Thus, actual SW may be larger than assumed by coupling model at lower afterload resistance and smaller at high afterload. Effect would be to shift E_a -to- E_{es} ratio at maximal measured SW to below 1.0. SEE, standard error of estimate.

afterloads), $P_{es} = SW/SV$ underestimates true P_{es} , whereas as resistance is reduced (declining P_{es}), the opposite is observed.

Several reports have suggested that the in situ heart and arterial system operate in a manner such that SW generation by the heart is maximal (6, 12, 14, 25–27). For example, in a recent study in the conscious chronically instrumented dog, Little and Cheng (12) found that the in vivo heart operates close to the point of maximal SW. This result is consistent with studies in anesthetized animals (4, 14, 26, 27). On the other hand, Piene and Sund (4) found in the cat right ventricle that metabolic efficiency and not SW appeared maximized. This observation is consistent with our previous theoretical prediction (3) and the recent observations by Sasayama et al. (1, 9, 19), who found E_a -to- E_{es} ratio of close to 0.5 in human subjects. These and other recent reports might be interpreted to indicate that metabolic efficiency, rather than SW, is optimized in intact circulations.

The present data provides an important perspective to the investigative search for what is or is not optimized under different conditions. Work and efficiency are both nearly maximal over a broad loading range, spanning physiological and pathophysiological values. Hence, we conclude that precise optimization of either parameter is likely of little consequence in the normal or moderately abnormal circulation. Instead, homeostasis in the intact system more likely centers on control of blood pressure, circulating volume, and oxygenation and can ignore ventricular SW or efficiency, since both should remain near maximal under many conditions. This built-in “safety net” is likely compromised only in severe ventricular or vascular disorders.

Experimental design. We recognize that one must be quite cautious when extrapolating isolated heart results to more intact or human data. However, it is nearly impossible to adequately measure the necessary variables without the controls afforded by the isolated-heart preparation. There are several specific aspects of the isolated-heart preparation that should be considered.

Coronary perfusion pressure was held constant, whereas in the intact circulation, this pressure would vary with ventricular-arterial interaction. This might reduce work at the lowest afterloads due to a fall in coronary perfusion pressure, making optimization curves appear less shallow. The contractile state of the isolated heart is often less than observed in situ. Because the optimum afterload resistance for metabolic efficiency ($SW/M\dot{V}O_2$) was affected directly by contractile state (Table 2), whereas this was not true for SW; the disparity between optimum afterload resistance for SW or $SW/M\dot{V}O_2$ in the intact circulation might be larger than appreciated from the current data. However, we expressly provided inotropic support in many of the runs so that the mean E_{es} was ~ 9.0 mmHg/ml, well within the range reported in conscious dogs (12). Lastly, the computer-simulated arterial impedance is a simplified model and does not encompass the full impedance characteristics of the natural arterial system.

The framework of elastance matching assumes that E_{es} is load independent. However, recent results from this

laboratory in the isolated blood-perfused canine heart (2), and others in the in situ heart (7, 8), indicate that ejection can yield an P_{es} that exceeds that predicted by a load-independent E_{es} . Specifically, we recently reported that reducing E_a in the isolated heart can result in an increase in E_{es} . Applying this to the present study would mean that as E_a is lowered, E_{es} might increase slightly, making the E_a -to- E_{es} ratio even lower than that calculated, assuming a fixed E_{es} . The opposite would hold for an increase in E_a . The effect would be to broaden the E_a -to- E_{es} vs. SW (or efficiency) relations even further. If anything, assuming a fixed E_{es} underplays the flat nature of these relations.

In conclusion, our study confirms that both SW and $SW/M\dot{V}O_2$ efficiency are optimal at a specific, but slightly different, ventricular-vascular coupling conditions. However, this difference is small, and the relations between SW or $SW/M\dot{V}O_2$ and coupling ratio are broad with considerable overlap. It would seem therefore unlikely that optimization of either parameter plays a major role in normal control of the circulation or ventricular-vascular coupling. Stated another way, homeostatic mechanisms can essentially ignore the heart without actively compromising its efficiency or external work.

The authors thank Kenneth Rent for excellent technical assistance during the experiments and Karen Augustine for secretarial assistance.

This work was supported by National Heart, Lung, and Blood Institute (NHLBI) Public Health Service Grant HL-18912, NHLBI Physician Scientist Award HL-01820 (to D. A. Kass), and fellowships from the American Heart Association, Maryland Affiliate (to D. Burkhoff and P. de Tombe). D. Kass is an Established Investigator of the American Heart Association.

Present address of P. de Tombe: Div. of Cardiology, Bowman Gray School of Medicine, Wake Forest University, Winston-Salem, NC 27103.

Address for reprint requests: D. A. Kass, Carnegie 538, The Johns Hopkins Hospital, 600 N. Wolfe St., Baltimore, MD 21205.

Received 24 July 1992; accepted in final form 23 December 1992.

REFERENCES

- Asanoi, H., S. Sasayama, and T. Kameyama. Ventriculo-arterial coupling in normal and failing heart in humans. *Circ. Res.* 65: 483–493, 1989.
- Burkhoff, D., P. P. de Tombe, W. C. Hunter, and D. A. Kass. Contractile strength and mechanical efficiency of left ventricle are enhanced by physiological afterload. *Am. J. Physiol.* 260 (*Heart Circ. Physiol.* 29): H569–H578, 1991.
- Burkhoff, D., and K. Sagawa. Ventricular efficiency predicted by an analytical model. *Am. J. Physiol.* 250 (*Regulatory Integrative Comp. Physiol.* 19): R1021–R1027, 1986.
- Elzinga, G., G. P. Toorop, D. R. Gross, and N. Westerhof. Geometry and pump function in cardiac ventricular hypertrophy. *Am. J. Cardiol.* 65: 23G–29G, 1990.
- Elzinga, G., and N. Westerhof. Pump function of the feline left heart: changes with heart rate and its bearing on the energy balance. *Cardiovasc. Res.* 14: 81–92, 1980.
- Elzinga, G., and N. Westerhof. Matching between ventricle and arterial load: an evolutionary process. *Circ. Res.* 68: 1495–1500, 1991.
- Freeman, G. L. Effects of increased afterload on left ventricular function in closed-chest dogs. *Am. J. Physiol.* 259 (*Heart Circ. Physiol.* 28): H629–H625, 1990.
- Igarashi, Y., C.-P. Cheng, and W. C. Little. Left ventricular ejection activation in the in situ heart. *Am. J. Physiol.* 260 (*Heart Circ. Physiol.* 29): H1495–H1500, 1991.
- Kameyama, T., H. Asanoi, S. Ishizaka, and S. Sasayama. Ventricular load optimization by unloading therapy in patients

- with heart failure. *J. Am. Coll. Cardiol.* 17: 199-207, 1991.
10. **Kass, D. A., and R. P. Kelly.** Ventriculo-arterial coupling: concepts, assumptions, and applications. *Ann. Biomed. Eng.* 20: 41-62, 1992.
 11. **Khalafbeigui, F. H., H. Suga, and K. Sagawa.** Left ventricular systolic pressure-volume area correlates with oxygen consumption. *Am. J. Physiol.* 237 (*Heart Circ. Physiol.* 6): H566-H569, 1979.
 12. **Little, W. C., and C.-P. Cheng.** Left ventricular-arterial coupling in conscious dogs. *Am. J. Physiol.* 261 (*Heart Circ. Physiol.* 30): H70-H76, 1991.
 13. **Motulsky, H. J., and L. A. Ransnas.** Fitting curves to data using non-linear regression: a practical and nonmathematical review. *FASEB J.* 1: 365-374, 1987.
 14. **Myhre, E. S. P., A. Johansen, J. Bjornstad, and H. Piene.** The effect of contractility and preload on matching between the canine left ventricle and afterload. *Circulation* 73: 161-171, 1986.
 15. **Nozawa, T., Y. Yasumura, S. Futaki, N. Tanaka, M. Uenishi, and H. Suga.** Efficiency of energy transfer from pressure-volume area to external mechanical work increases with contractile state and decreases with afterload in the left ventricle of the anesthetized dog. *Circulation* 77: 1116-1124, 1988.
 16. **Piene, H., and T. Sund.** Does normal pulmonary impedance constitute the optimum load for the right ventricle? *Am. J. Physiol.* 242 (*Heart Circ. Physiol.* 11): H154-H160, 1982.
 17. **Sagawa, K., L. Maughan, H. Suga, and K. Sunagawa.** *Cardiac Contraction and the Pressure-Volume Relationship.* New York: Oxford Univ. Press, 1988.
 18. **Sarnoff, S. J., E. Braunwald, G. H. Welch, R. B. Case, W. N. Stainsby, and R. Macruz.** Hemodynamic determinants of oxygen consumption of the heart with special reference to the tension-time index. *Am. J. Physiol.* 192: 148-156, 1958.
 19. **Sasayama, S., and H. Asanoi.** Coupling between the heart and arterial system in heart failure. *Am. J. Med.* 90, *Suppl.*: 14S-18S, 1991.
 20. **Schroff, S. G., K. T. Weber, and J. S. Janicki.** Coupling of the left ventricle with the arterial circulation. In: *McDonald's Blood Flow in Arteries*, edited by W. W. Nichols and M. F. O'Rourke. Philadelphia, PA: Lea & Febiger, 1990, p. 343-359.
 21. **Suga, H.** Total mechanical energy of a ventricular model and cardiac oxygen consumption. *Am. J. Physiol.* 236 (*Heart Circ. Physiol.* 5): H498-H505, 1979.
 22. **Suga, H., and K. Sagawa.** Instantaneous pressure-volume relationships and their ratio in the excised, supported canine left ventricle. *Circ. Res.* 35: 117-126, 1974.
 23. **Sunagawa, K., D. Burkhoff, K. O. Lim, and K. Sagawa.** Impedance loading servo pump system for excised canine ventricle. *Am. J. Physiol.* 243 (*Heart Circ. Physiol.* 12): H346-H350, 1982.
 24. **Sunagawa, K., W. L. Maughan, D. Burkhoff, and K. Sagawa.** Left ventricular interaction with arterial load studied in isolated canine ventricle. *Am. J. Physiol.* 245 (*Heart Circ. Physiol.* 14): H773-H780, 1983.
 25. **Sunagawa, K., W. L. Maughan, and K. Sagawa.** Optimal arterial resistance for the maximal stroke studied in isolated canine left ventricle. *Circ. Res.* 56: 586-595, 1985.
 26. **Toorop, G. P., G. J. Van den Horn, G. Elzinga, and N. Westerhof.** Matching between feline left ventricle and arterial load: optimal external power or efficiency. *Am. J. Physiol.* 254 (*Heart Circ. Physiol.* 23): H279-H285, 1988.
 27. **Van den Horn, G. J., N. Westerhof, and G. Elzinga.** Optimal power generation by the left ventricle. A study in the anesthetized open thorax cat. *Circ. Res.* 56: 252-261, 1985.
 28. **Wilcken, D. E. L., A. A. Charlier, J. I. E. Hoffman, and A. Guz.** Effect of alterations in aortic impedance on the performance of the ventricles. *Circ. Res.* 14: 283-293, 1964.

